This is not a peer-reviewed article.
Pp. 357-366 in Automation Technology for Off-Road Equipment, Proceedings of the July 26-27, 2002 Conference (Chicago, Illinois, USA) Publication Date July 26, 2002. ASAE Publication Number 701P0502, ed. Qin Zhang.

Control and Evaluation Methods for Multi-Mode Steering

Mitchell A. Miller and Brian L. Steward[1]

ABSTRACT

A self-propelled agricultural sprayer was modified to enable both front and rear wheel steering through electrohydraulic control valves. These modifications, in conjunction with a digital controller, enabled the vehicle to be four-wheel steered in multiple modes. The research focused on modeling and evaluating the effect of multi-mode four-wheel steering on vehicle handling characteristics and vehicle performance of the sprayer. The multi-mode steering system was evaluated by driving the sprayer through specified paths in the different steering modes. The position and heading of the vehicle were measured for each mode using two dual frequency DGPS receivers. From the measure of vehicle posture, sprayer performance measures such as over/underspray and crop damage were assessed for each steering mode. Preliminary results show that drivers were able to take advantage of added maneuverability in headland turning procedures. Crab steering reduced the amount of area sprayed in error during lateral course adjustments. The steering and vehicle models yielded similar responses to steering inputs as experimental responses.

KEYWORDS. Vehicle performance. Steering control. Vehicle modeling.

INTRODUCTION

Self-propelled agricultural sprayers are being designed with boom lengths exceeding 30 m (100 ft) and field speeds of nearly 9 m/s (20 mph). These two parameters, along with the trend towards automatic guidance of sprayers, make vehicle control of utmost importance. In this research, a self-propelled agricultural sprayer was modified to enable four-wheel steering using electrohydraulic control valves. This enabled the vehicle to be steered in multiple modes. The research focused on evaluating the effect of multi-mode four-wheel steering on vehicle handling characteristics and vehicle performance of the sprayer. This paper describes multi-mode steering implementation, steering system and vehicle modeling, and vehicle performance evaluation.

The concept of four-wheel multi-mode steering on agricultural vehicles is not new. The J.I. Case Company produced multi-mode steered four-wheel drive tractors from 1964 to the early 1990's (Wendel, 1991). The Case tractors used an analog solid-state selective steering control system with four modes: coordinated steering, conventional steering, crab steering and independent rear steering (Lourigan and Patel, 1979). Cullman (1985) described a similar system that used analog electronics and proportional hydraulic components to achieve multi-mode steering. Myers and Gillespie (1977) developed a hydraulic system to achieve four-wheel steering on a papaya harvester. In this system, a solenoid valve activated by two switches hydraulically connected the rear steering cylinder in series with the front steering cylinder. The solenoid DCV was also used to switch from crab to coordinated rear wheel steering. Four-wheel steering can also be accomplished through a mechanical linkage, as implemented in a farm transport vehicle described by Dwyer and Wheeler (1987). Itoh and Oida (1990) described a Japanese tractor using a mechanical linkage that switched from one crab steering to coordinated four-wheel steering when the steering wheel was rotated through an angle greater than 200 degrees.

---

[1] The authors are Mitchell A. Miller, Operations Management Associate, General Mills, Great Falls, Montana, and Brian L. Steward, Assistant Professor, Agricultural and Biosystems Engineering Department, Iowa State University, Ames, Iowa, email: <bsteward@iastate.edu>.

The objectives of this research were to implement four-wheel multimodal steering on an agricultural sprayer, model the steering system and vehicle, and evaluate the effect of four-wheel steering on vehicle performance. Three modes of steering were evaluated: steering the front wheels only (conventional steering), steering all four wheels in the same direction (crab steering), and steering the rear wheels in the opposite direction of the front wheels (coordinated steering) (Figure 1). However, the steering system was not limited to these three modes, as any

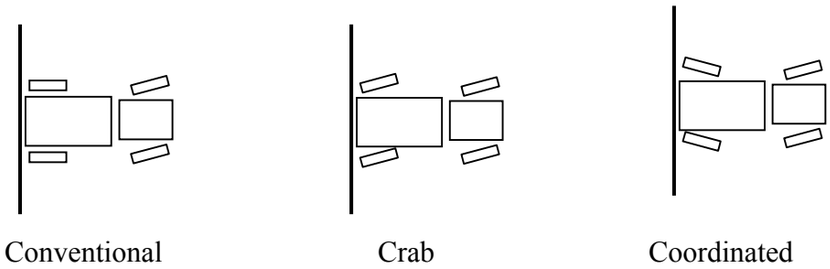

Figure 1. With four-wheel steering, three modes of steering exist: conventional, crab and coordinated.

combination of front and rear wheel steering angles could be achieved by the system. For this research, the system was constrained to use only three modes to make the experimental design manageable.

CONTROLLER METHODS AND MATERIALS

Control Valves and Sensor Hardware

A John Deere 4710 sprayer was modified to include a rear axle that had steerable wheels and associated steering cylinders. Each steerable wheel was equipped with a non-contact rotary potentiometer sensor to measure steering angle. The sensor was mounted on the ball joint on the rod end of the cylinder. A linkage was used to connect the armature of sensor to the sprayer steering linkage. The sensors were calibrated by measuring the sensor voltage output as the steering cylinders were extended in half-inch increments. From cylinder extension, the steering angle was determined (Figure 2). The calibration points were then plotted on a graph and a third order curve was used to approximate the plot of steering angle vs. sensor voltage.

Two Sauer Danfoss PVG 32 control valves were controlled with a signal that was a proportion of the supply voltage. The valve for the front wheels could be actuated by either a hydraulic pilot pressure provided by the steering unit at the steering wheel or electrically. The front wheels were controlled hydraulically through the steering wheel for the evaluations described in this

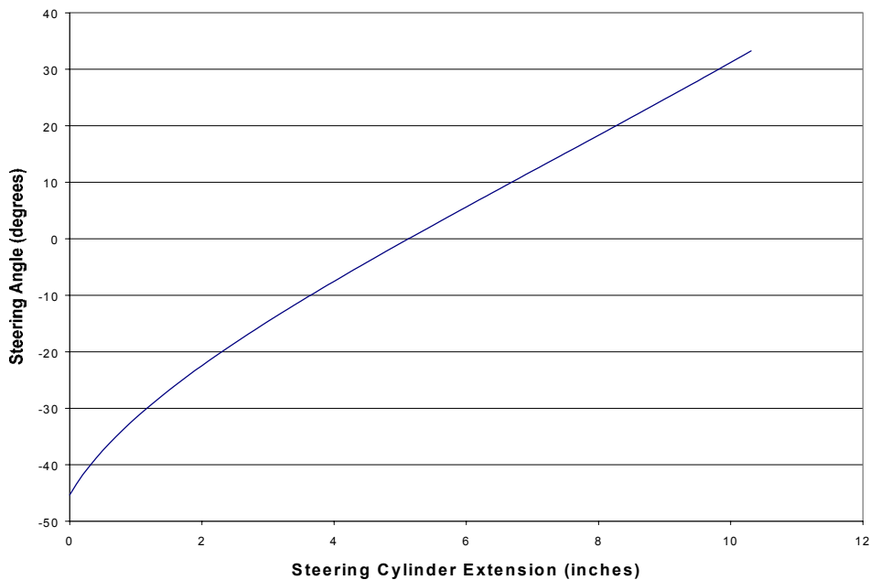

Figure 2. Kinematic relationship between steering cylinder rod position and steering angle for the sprayer vehicle.

paper. The rear valve could only be controlled electrically. The PVG 32 control offered a linear response with pressure compensation and a narrow deadband region. The valve characteristic eliminated many of the problems and subsequent analysis encountered in much of the previous electrohydraulic steering research that has focused on modeling and controlling nonlinear hydraulic directional control valves (Qui et al., 1999).

Controller Hardware and Algorithm

A microprocessor-based, expandable controller (Smart Star 9000, Z-World, Davis, CA) was used to control the steering system and provide a user interface. The controller was a modular and expandable control system with a 25.8 MHz CPU card installed on a back plane. The back plane had expansion ports containing a digital I/O card, an A/D card and a D/A card. The controller was programmed using Dynamic C Premier (Z-World, Davis, CA), which is a modified C language with libraries to program the controller. A switch with a LED numeric display allowed the user to select the steering mode and indicate the steering mode that was currently being used.

Two control algorithms were developed for this project. For the first control algorithm (Figure 3a), the driver provided a steering input through the steering wheel. The steering hand pump then provided a hydraulic pilot signal to the steering valve, and the front wheels were positioned accordingly. The signal from the front steering angle sensors was used as the set point for the proportional controller, which closed the loop around the rear E/H steering valve, hydraulic cylinder and mechanical linkage. Steering modes were implemented in software by multiplying the front steering angle signal by 1, 0, or -1 to achieve crab, conventional, or coordinated steering respectively. In the second control algorithm (Figure 3b), a PC commanded a steering angle set point to both the front and rear wheels. The controller then implemented closed-loop control to both the front and rear steering systems with modes implemented similarly as the first algorithm.

For each steering algorithm, the controller program sampled the mode setting every 0.1 s. The output of each steering angle sensor was sampled every 0.01 s. Sensor outputs were related to steering angles through calibration curves, and the average steering angle of each set of front or rear wheels was used for steering error calculations. Proportional control was used with dead band compensation.

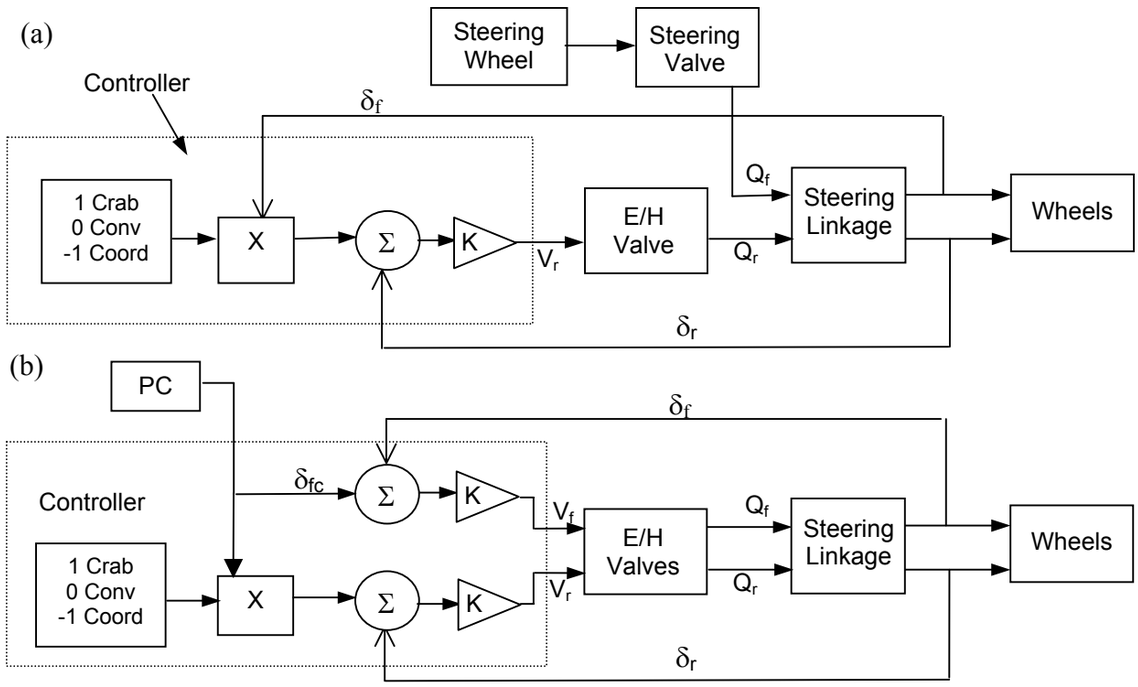

Figure 3. (a) Block diagram of the closed loop control system for sprayer vehicle with computer input. (b) Block diagram of the E/H steering system for sprayer vehicle with steering wheel input.

Data Acquisition

A 12-bit analog resolution data acquisition system (DaqBook 120, IOTech, Cleveland, OH) was used to acquire wheel angle data. The voltage output of the four steering angle sensors and the input voltage to the directional control valves were recorded by the data acquisition system.

Vehicle posture was measured at a 5 Hz update rate using two dual frequency DGPS receivers (StarFire, John Deere, Moline, IL) mounted along the centerline of the vehicle 3.8 m (12.5 ft) apart. The GPS receivers achieved an accuracy of about ± .3 m (1 ft) in the field over long periods of time. For time periods of less than fifteen minutes, the relative error between the two receivers was consistent, and therefore could be removed through calibration. To calibrate the GPS receivers, the sprayer was driven directly north and directly east at the beginning of each experimental replication to determine the bias, and the bias was subtracted from the front receiver location data in a post-processing procedure.

STEERING AND VEHICLE MODELS

A dynamic vehicle model was developed in order to better understand the vehicle dynamics and to be able to predict how the vehicle will respond to inputs. A dynamic model of the steering controller and sprayer vehicle was developed in order to approximate the vehicle response to steering inputs.

Dynamic Vehicle Model

The dynamic vehicle model was developed using the yaw plane and bicycle model. This allowed for the application of the two-degrees of freedom equations (Ellis, 1994, Gillespie, 1992). The bicycle model allowed the left and right wheel angles to be represented by an equivalent average steering angle of both wheels (Figure 4). The cornering force generated by the one wheel was then equivalent to the sum of the force on the left and right wheels. The bicycle model was valid for relatively small steer angles (about 10 degrees) where the angles of the left and right wheels were approximately equal.

The dynamic model takes into account the lateral forces at the front and rear wheels, the mass of the vehicle, the mass moment of inertia of the vehicle and the location of the center of gravity. The mass moment of inertia of the vehicle was estimated using a rectangular model of the vehicle. A nonlinear tire model (Miller, 2001) was used to find the forces on the front and rear wheels based on the slip angles of the wheels.

The dynamic vehicle model had two degrees of freedom: lateral translation and rotation. The dynamic vehicle model equations (shown below) were derived from Newton's laws of motion. The translational equation (Eq. 1) shows that the rate of change of lateral velocity of the vehicle is a function of the lateral forces on the front and rear tires as well as the yaw rate of the vehicle. The rotational equation shows that the yaw acceleration is the sum of moments about the center of gravity of the vehicle divided by the moment of inertia about the center of gravity of the vehicle (Eq. 2). The sideslip angle of the center of gravity is a function of the ratio of lateral vehicle velocity to forward vehicle velocity (Eq. 4). For this model, the forward vehicle velocity was assumed constant, a valid assumption for small sideslip angles. The slip angles of the tires are a function of the slip angle of the vehicle and the steering angle of tires (Eq. 5 and 6). The velocity component of the front and rear of the vehicle caused by the yaw rate of the vehicle was also included in the slip angle equations. Mathematically:

$$\dot{v} = \left(\frac{F_f \cos\delta_f + F_R \cos\delta_R}{m_v} \right) - u \cdot r \qquad (1)$$

$$\dot{r} = \frac{\left(F_f \cos\delta_f\right) \cdot a - \left(F_R \cos\delta_R\right) \cdot b}{I_{zcg}} \qquad (2)$$

$$\psi = \int r \cdot dt + \psi_0 \qquad (3)$$

$$\beta = \tan^{-1}\left(\frac{v}{u}\right) \tag{4}$$

$$\alpha_f = \left(\left(\frac{v + a \cdot r}{u}\right) - \delta_f\right) \tag{5}$$

$$\alpha_r = \left(\left(\frac{v - b \cdot r}{u}\right) - \delta_r\right) \tag{6}$$

$$y = \int u \cdot \sin(\psi + \beta) \cdot dt + y_0 \tag{7}$$

$$x = \int u \cdot \cos(\psi + \beta) \cdot dt + x_0 \tag{8}$$

where :

x = x coordinate of vehicle in World Coordinate System (m)

y = y coordinate of vehicle in World Coordinate System (m)

v = lateral velocity of vehicle center of gravity (m/s)

u = forward velocity of vehicle center of gravity (m/s)

r = yaw rate of center of gravity (rad/sec)

β = sideslip angle of center of gravity (radians)

ψ = angle of orientation of vehicle in WCS (radians)

α_f, α_r = slip angle of front and rear wheels, respectively (radians)

a = distance from front axle to center of gravity (m)

b = distance from rear axle to center of gravity (m)

δ_f = average steering angle of front wheels (radians)

δ_R = average steering angle of rear wheels (radians)

F_f = cornering force on front wheels (N)

F_R = cornering force on rear wheels (N)

m_v = total mass of the vehicle (kg)

I_{zcg} = mass moment of inertia about the center of gravity ($kg \cdot m^2$)

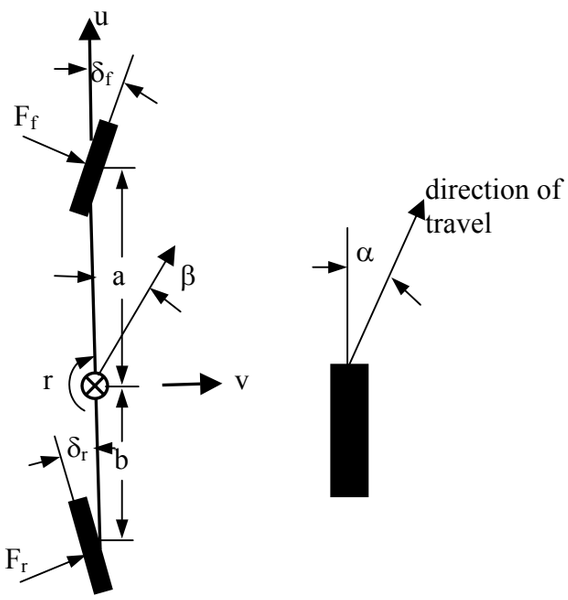

Figure 4. Location of dynamic vehicle variables on the vehicle bicycle model.

Steering System Model

The steering system was modeled to provide realistic steering angle inputs to the vehicle models. The linear characteristics of the pressure compensated E/H proportional steering valves allowed it to be linearly modeled outside the dead band using a gain of 9.1 L/min/V. The steering cylinders were modeled using the fluid continuity law with the assumption of fluid incompressibility. Thus extension velocity of the cylinder was related to fluid flow into the cylinder. The kinematic relationship for the steering angle as a function of the extended length of the cylinder was developed from the geometry of the steering linkage.

Model Validation

To validate the model, the vehicle was operated under field conditions, and the experimental results were compared to simulations using the model. The first test of the model was to determine the steering angle response to a step input to the front and rear steering valves. This was done to determine how accurately the valve and controller model simulate the actual controller and steering valves. A square wave input of 38 degrees at a frequency of 0.125 Hz was entered into the simulation and tested in the field. The sprayer vehicle was tested for this input with the tank empty and the boom folded, traveling at about 3 mph. The second test of the model examined the vehicle response of the vehicle steering inputs. A square wave steering angle with amplitude of 10 degrees and frequency of 0.125 Hz was input to the front and rear steering valves in the coordinated steering mode with the sprayer vehicle traveling 8 mph. The position of both the front and rear of the sprayer was measured and compared with the response of the dynamic vehicle model.

EVALUATION METHODS

In order to justify the additional cost required to implement 4-wheel multi-mode steering, there must be evidence that vehicle performance associated with 4-wheel steering will bring benefit to the end user. Three tests were therefore developed to quantitatively evaluate the effect of multi-modal steering on vehicle performance. These tests were intended to determine how much added maneuverability from 4-wheel steering could be used by the driver in typical field maneuvers.

Effective Turning Radius

The smallest effective turning radius for both conventional and coordinated steering was measured when the vehicle was moving at about 0.5 m/s (1 mph) with the wheels turned to the maximum angle. The effective turning radius was determined by measuring the distance from the center of the turning circle to the center of the rear axle for conventional steering. For coordinated steering the effective turning radius was determined by measuring the distance from the center of the turning circle to the center of the vehicle.

Smallest effective turning radii were measured on three different surfaces: pavement, loose soil and established grass. For the measurement on pavement, the tires were sprayed with a soap solution so the wheel tracks were visible. On the other surfaces, the wheels left a mark in the soil. GPS was also used to measure turning radii and was found to give equivalent measurements to manual measurements.

Headland Performance

The time and space required to turn around at the end of a field is directly related to field efficiency. Crop damage caused by wheel tracks in the headlands is directly related to total field production. Thus the added maneuverability of four-wheel steering should improve headland-turning performance. Headland performance was quantified in three ways: the distance required for the vehicle to align with the rows before reentering the crop, the headland width required for turning, and the total damaged crop area during a turn. To measure the headland performance of two-wheel conventional steering and four-wheel coordinated steering, two parallel paths, 45.7 m (150 ft) long and 27.4 m (90 ft) apart were set up using field marking flags to simulate field rows (Figure 5a). The first path was followed until the boom reached the end of the path. At this

point the vehicle was turned sharply to establish a vehicle heading perpendicular to the paths. When the vehicle neared the second path, it was turned sharply again to direct it down the second path. This procedure was repeated at both ends of the paths with the entire loop traveled five times for each mode of steering. The test was repeated for two drivers to examine the effect of driver-to-driver differences. This test was performed with the boom extended on both loose soil and on established grass at speeds between 1.6 and 1.8 m/s (3.5 to 4.0 mph).

The distance required for the vehicle to align with the rows was determined by measuring the distance from start of the crop rows to the center of the boom when the sprayer was aligned with the rows to within the error level. The width required to turn around was determined by measuring the distance from the end of the rows to the tip of the outside boom. The wheel track area was assumed to be the area where potential crop damage would occur. This area was found by calculating the distance of each wheel track during the entire turn and multiplying the distance by the tire width. Where at least 50 percent of a rear wheel track was on top of a front wheel track, the two tracks were considered one track. The wheel tracks were determined from the GPS location measurements. These measurements were verified by physically measuring the wheel tracks for random GPS samples.

Lateral Path Adjustment

When lateral course corrections are necessary, it is important to minimize spray skip and overlap, over/underspray, and crop damage. A test was developed to measure the performance of the sprayer vehicle in each of the three steering modes while performing a lateral path adjustment. Two 76 m (250 ft) long paths were set up parallel with each other 3.8 m (12.5 ft) apart. The paths were marked out in the field using marking flags spaced 7.6 m (25 ft) apart. The first path was followed for 15 m (50 ft); then the sprayer was guided to the second path and followed the second path until the 46 m (150 ft) mark; then the sprayer was returned to the first path for the last 30 m (100 ft) of the path (Figure 5b). GPS measurement of vehicle posture was used to calculate the movement of the boom during course adjustments. From estimates of boom movement, undersprayed or oversprayed areas were calculated and used as a performance

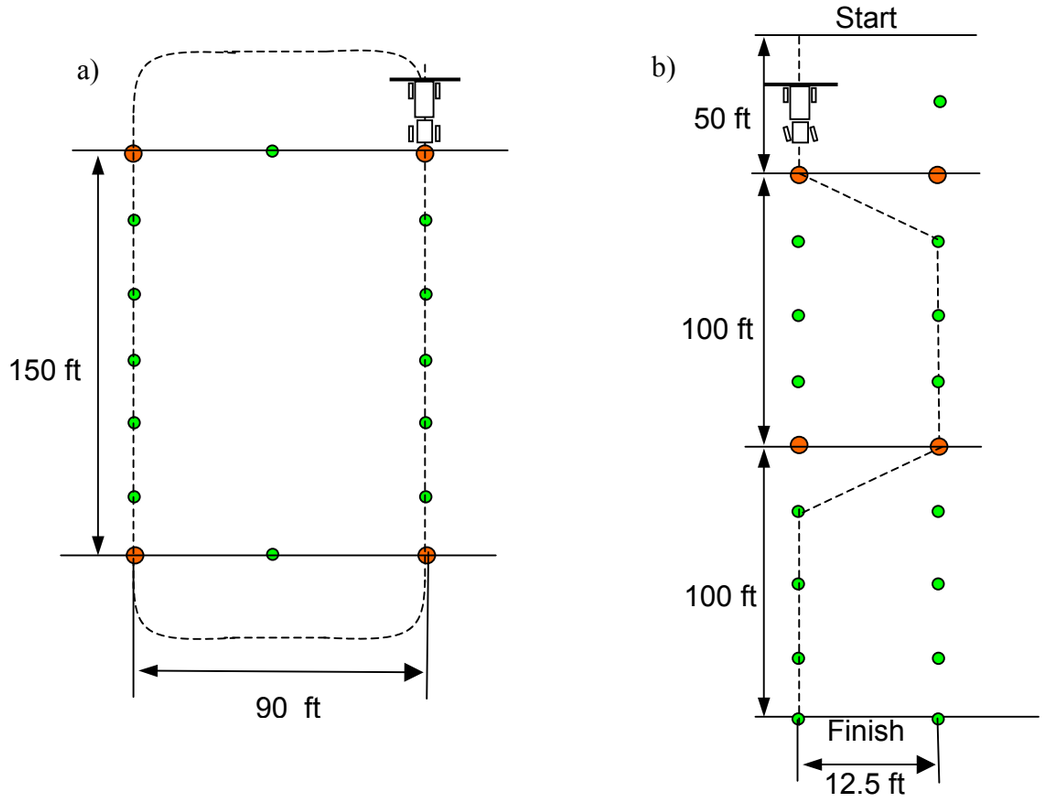

Figure 5. Illustrations of test paths: a) headland performance test path. b) lateral path adjustment test path. Dots indicate location of flags.

measure. This test was repeated by three different drivers and on two different soil conditions, established grass and loose soil. Each driver repeated the test six times in each mode of steering. All tests were conducted with the boom fully extended, with 570 liters (150 gallons) of water in the tank, and a vehicle speed of 2.7 m/s (6 mph).

RESULTS

Steering Angle Response

In simulation, the wheels responded from zero to full right in about 0.9 seconds, while experimentally, the wheels took about 1.3 seconds to turn full right (Figure 6). Two assumptions made in this model may have contributed to the error. The model assumed that there was no lag between the arrival of the signal at the valve and valve opening. In reality, there is a finite time associated with the valve opening. Another assumption was that the valve was the only limiting flow factor, but it appeared that there was another limiting factor. The slope of the line from the field test showed that the actual flow out of the valves (16.7 L/min) was about 2/3 of the maximum flow rate through the valves (24.2 L/min). Using this flow rate in the simulation produced a response that better matched the actual vehicle response.

Vehicle Response

The dynamic vehicle model performed well in simulating the vehicle position in time based on steering inputs and vehicle velocity. Vehicle trajectories for the simulation and field test are shown in Figure 7. The starting orientation and location of the vehicle in the field test and that of the simulation were synchronized as best as possible, but not perfectly, accounting for some of the error. Figure 8 shows a plot of yaw rates for the dynamic simulation and for the field test. This plot may be a better representation of how well the model simulated the actual vehicle response, as the yaw rate was independent of the vehicle orientation and starting location.

Performance Evaluation

From preliminary results, we found that the turning radius achieved with coordinated steering was about half that of conventional steering on all different surfaces. This increased maneuverability reduced the headland width required for turning around and increased the distance available to align the vehicle with crop rows. Crab steering had the least amount of under/oversprayed areas when making a lateral path adjustment (Figure 9). The difference

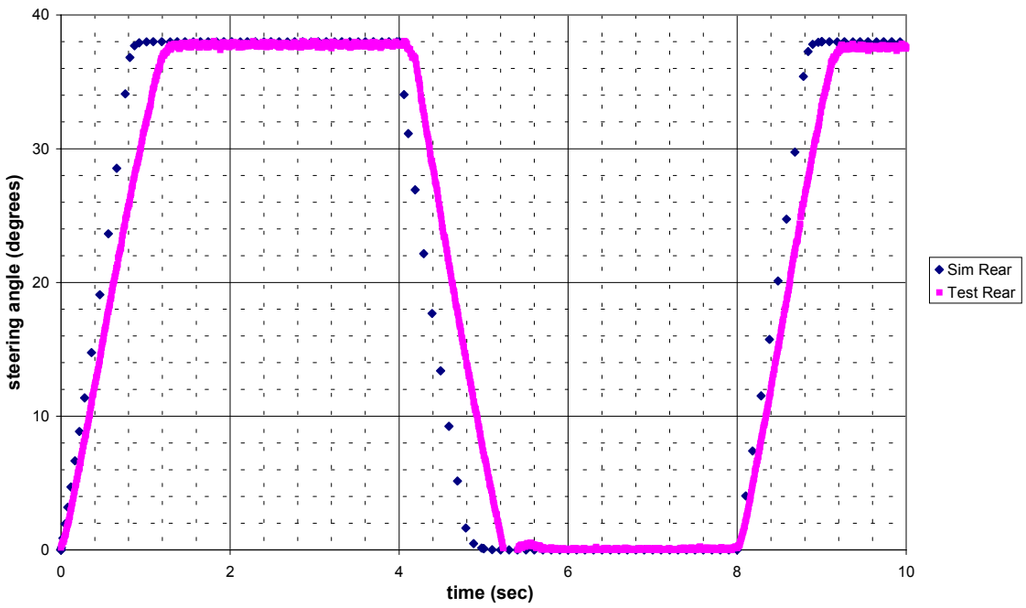

Figure 6. Plot of simulated steering response of wheels to step input in steering angle assuming full flow through valves and plot of actual wheel response on vehicle.

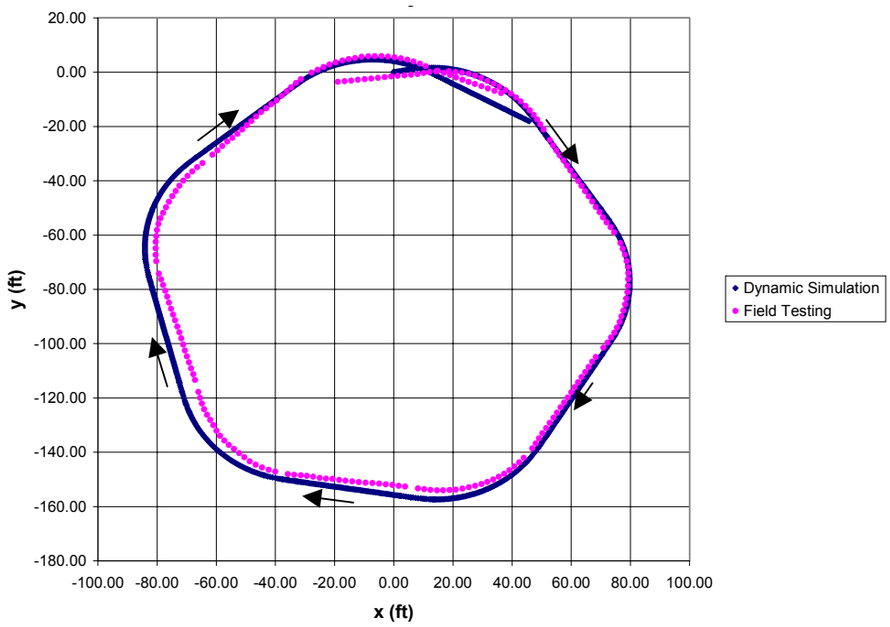

Figure 7. Plot of x vs. y for dynamic simulation and field test for a square wave input of 10 degrees steering angle at 8 mph in coordinated steering.

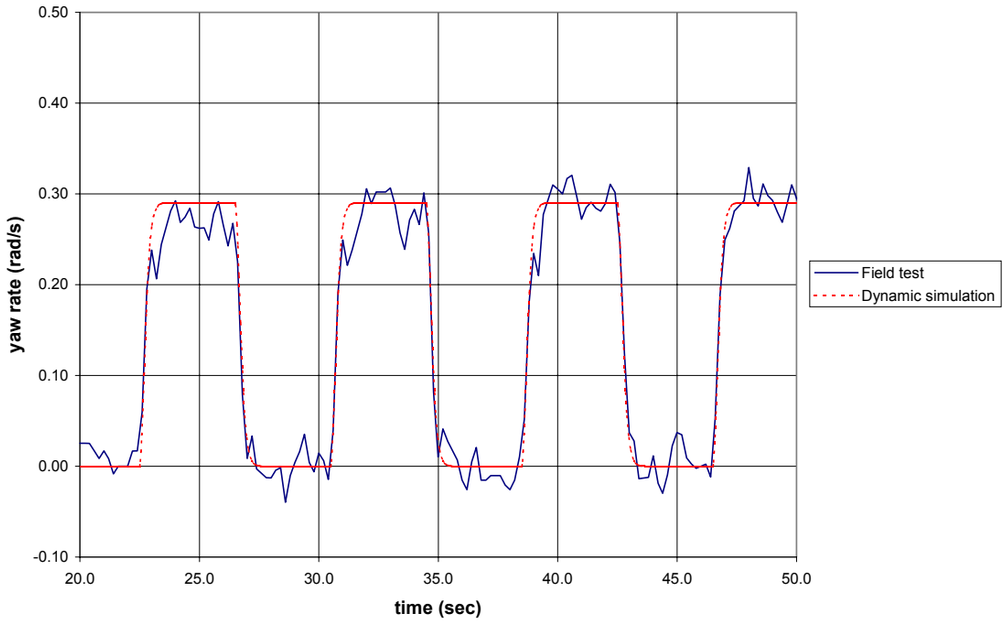

Figure 8. Plot of yaw rate vs. time for dynamic model simulation and field test for a square wave input of 10 degrees steering angle at 8 mph in coordinated steering.

between conventional and coordinated steering modes was not statistically significant and was dependent on the drivers' experience.

CONCLUSION

In conclusion, the steering controller provided robust, repeatable results with processing times much faster than the valve dynamics. In the master-slave control scheme, the rear wheels lagged the front wheels by about two to three degrees when the steering wheel was turned at a fast rate. Four-wheel steering not only increased vehicle maneuverability, but operators were also able to use this maneuverability in common field operations. Simulations from the steering system and vehicle model correlated well with experimental results.

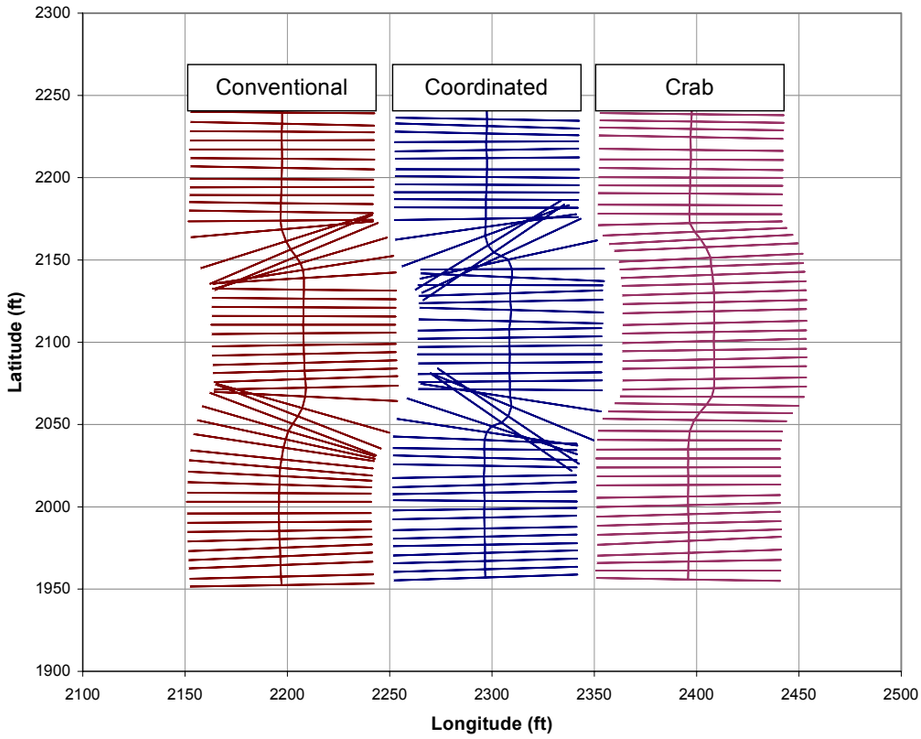

Figure 9. Estimated boom positions during the lateral path adjustment test in three different modes of steering.

Acknowledgments

The authors would like to thank Deere and Co. for their support of this research and Sauer-Danfoss for their technical support throughout the project.

REFERENCES

1. Cullman, J. 1985. Multi-Mode Electrohydraulic Steering System for Off-Road Vehicles. SAE Paper No. 85-1491. Warrendale, PA: SAE.
2. Dwyer, M. J. and J. A. Wheeler. 1987. Preliminary results from the on-farm evaluation of an experimental farm transport vehicle. *Journal of Agricultural Engineering Research* 38: 15-26.
3. Ellis J. R. 1994. *Vehicle Handling Dynamics*, Mechanical Engineering Publications Limited: London, England.
4. Gillespie, T. 1992. Fundamentals of Vehicle Dynamics, SAE. Warrendale, PA.
5. Itoh, H. and A. Oida. 1990. Dynamic analysis of turning performance of 4WD-4WS tractor on paved road. *Journal of Terramechanics* 27(2): 125-143.
6. Lourigan, P. and Patel, K. 1979. Agricultural Tractor Elector-Hydraulics. SAE Paper No. 79-0848. Warrendale, PA: SAE.
7. Miller, M. A. 2001. Development and evaluation of multi-mode four-wheel electrohydraulic steering system on a sprayer vehicle. Thesis, Iowa State University: Ames, IA.
8. Myers, A.L. and Gillespie, B.A. 1979. Electrohydraulic Device for Shifting from Four to Two-Wheel Steering. *Transaction of the ASAE* 20(2): 258,261.
9. Qui, H., Q. Zhang, J. F. Reid, and D. Wu. 1999. Modeling and Simulation of an Electrohydraulic Steering System. ASAE Paper No. 99-3076. St. Joseph, MI: ASAE.
10. Wendel, C. H. 1991. *150 Years of J.I. Case.* Sarasota, FL: Crestline Publishing Co.